Pharmaceutical stabilization of abdominal aortic aneurysms : changing its natural history

Kokje, V.B.C.

Chapter 9

ADVENTITIAL ADIPOGENIC DEGENERATION IS AN UNIDENTIFIED CONTRIBUTOR TO AORTIC WALL WEAKENING IN THE ABDOMINAL AORTIC ANEURYSM

Stefan A. Doderer[1], Gabor Gäbel[2], Vivianne B.C. Kokje[1], Bernd H. Northoff[3], Lesca M. Holdt[3], Jaap F. Hamming[1], Jan H.N. Lindeman[1]

[1] Department of Vascular Surgery, Leiden University Medical Center, Leiden, The Netherlands
[2] Department of Vascular and Endovascular Surgery, Ludwig-Maximilians-University Munich, Munich, Germany
[3] Institute of Laboratory Medicine, Ludwig-Maximilians-University Munich, Munich, Germany

Accepted in the Journal of Vascular Surgery

ABSTRACT

Objective

The processes driving human abdominal aortic aneurysm progression are not fully understood. While anti-inflammatory and proteolytic strategies effectively quench aneurysm progression in preclinical models, so far all clinical interventions failed. These observations hint at incomplete understanding of processes involved in abdominal aortic aneurysm progression and rupture. Interestingly, strong clinical and molecular associations exist between popliteal artery aneurysms and abdominal aortic aneurysms however, popliteal artery aneurysms have an extremely low propensity to rupture. We thus reasoned differences between these aneurysms may provide clues towards (auxiliary) processes involved in abdominal aortic aneurysm-related wall debilitation. A better understanding of the pathophysiologic processes driving abdominal aortic aneurysm growth can contribute to pharmaceutical treatments in the future.

Methods

Aneurysmal wall samples were collected during open elective and emergency repair. Control peri-renal aorta was obtained during kidney transplantation, and reference popliteal tissue obtained from the anatomy department. This study incorporates various techniques including (immuno) histochemistry, Western Blot, quantitative polymerase-chain-reaction, microarray and cell culture.

Results

Histological evaluation of abdominal aortic aneurysms, popliteal artery aneurysms and control aorta shows extensive medial (popliteal artery aneurysm) and transmural fibrosis (abdominal aortic aneurysm), and reveals abundant adventitial adipocytes aggregates as an exclusive phenomenon of abdominal aortic aneurysms (P<.001). qPCR, IHC, Western blotting and microarray analysis showed enrichment of adipogenic mediators (C/EBP family P=.027; KLF5 P<.000; and PPAR- P=.032) in abdominal aortic aneurysm tissue. *In vitro* differentiation tests indicated a sharply increased adipogenic potential of abdominal aortic aneurysm adventitial mesenchymal cells (P<.000). Observed enrichment of adipocyte related genes and pathways in ruptured abdominal aortic aneurysm (P<.000) supports an association between the extent of fatty degeneration and rupture.

Conclusion

This translational study identifies extensive adventitial fatty degeneration as an ignored and distinctive feature of abdominal aortic aneurysm disease. Enrichment of adipocyte-genesis and adipocyte-related genes in ruptured AAA point to an association between the extent of fatty degeneration and rupture. This observation may (partly) explain the failure of medical therapy and could provide a lead for pharmaceutical alleviation of abdominal aortic aneurysm progression.

INTRODUCTION

An abdominal aortic aneurysm (AAA) is a localized, progressive dilatation of the terminal aortic segment. If left untreated, AAA's will rupture and a ruptured AAA constitutes a prominent cause of sudden death in elderly males.[1]

At this point the pathophysiology of AAA growth and ultimately rupture remains an enigma.[2] The prevailing concept is that aneurysm progression is essentially driven by a localized pro-inflammatory response and accompanying proteolytic imbalance; the latter being held responsible for a progressive, and ultimately fatal weakening of the vessel wall.[3, 4]

Remarkably, while interference with inflammatory and/or proteolytic cascades proves highly effective in animal models of the disease, all clinical studies so far fail to show a benefit.[5-10] In fact, against all expectations interference with aspects of inflammation in the clinical setting may even accelerate disease progression.[11, 12] Altogether these clinical observations suggest that factors beyond proteases and inflammation are involved in progression (and rupture) of human AAA.

Remarkable strong clinical and molecular associations exist between AAA and popliteal artery aneurysms (PAA).[3] Yet, while the natural history of AAA is that of rupture, the primary concern in PAA's is thrombosis and rupture is rare in the context of PAA.[13] Hence, we reasoned that inherent differences between these two forms of aneurysms may provide clues towards auxiliary processes contributing to AAA wall rupture. On this basis we considered a patho-histological (re-)examination of AAA and PAA wall samples relevant.

Results of this evaluation identify extensive adventitial adipocyte accumulation as a thus far unrecognized feature that distinguishes growing AAA from PAA. In this paper we explore fatty degeneration as an novel additional pathophysiologic mechanism in AAA, and test a possible association between the process and terminal aortic wall weakening (rupture) in the disease.

MATERIALS AND METHODS

Tissue samples

All tissue samples were obtained from the Vascular Tissue Bank at the Department of Vascular Surgery, Leiden, the Netherlands. AAA and PAA samples were collected during elective and emergency aneurysm repair. Reference (non-aneurysmal) infra renal abdominal aortic wall samples were obtained during clinical organ transplantation from unused donor aortic tissue.[14] Considering the ample presence of atherosclerotic lesions in AAA wall samples, we specifically selected donor specimens with advanced atherosclerotic disease (viz. all samples selected had earlier[14] been classified as late fibroadenoma or higher (Modified AHA classification according to Virmani))[15] as reference (control) tissue.

Reference popliteal artery samples were kindly donated by the department of human anatomy. Movat staining of these popliteal samples did not indicate intermediate or advanced atherosclerotic lesions. Sample collection and handling was performed in accordance with the guidelines of the Medical and Ethical committee in Leiden, The Netherlands and the code of conduct of the Dutch Federation of Biomedical Scientific Societies (https://www.federa.org/codes-conduct).

Handling of the aneurysmal tissues was as follows: after obtaining tissue specimens, the adhering thrombus was carefully removed and tissue divided in three sections. One section was fixed in

formaldehyde (4%) for 24h, and decalcified in Kristensen's solution for 120h followed by embedding in paraffin. A second section was snap frozen in liquid nitrogen and stored at -80°C to be used for mRNA and protein analysis. The third section was kept in NaCl 0.9% and adventitial mesenchymal cells were isolated within 24h. For this purpose tissue was split along the medial-adventitial border and the adventitial segment used for cell isolation.

Histology and Immunohistochemistry

Histochemistry and immunohistochemistry (IHC) was performed on 4µm thick tissue sections. Slides were deparaffinized using xylene followed by rehydration. Histologic evaluation of vessel wall architecture was performed using Movat's pentachrome and Sirius Red staining according to local protocols. IHC was performed using heat induced epitope retrieval (HIER) combined with overnight incubation of primary antibodies. Antibodies against KLF-5 (AF3758, R&D Systems, Abingdon, United Kingdom) and PPAR- (AHP1461, AbdSerotec, Puchheim, Germany) were diluted to 1:200 and 1:1000 in 1% BSA respectively. Envision detection system (Dako, Amsterdam, The Netherlands) was used as secondary antibody. Samples were stained with DAB (Dako, Amsterdam, The Netherlands), and counterstained with Mayer's hematoxylin (Merck Millipore, The Netherlands). For quantification purposes one full length section (typically 10-15 mm) per patient was quantified. Stained slides were scanned at 400x magnification using Philips' IntelliSite Ultra Fast Scanner (Philips, Eindhoven, the Netherlands) and representative sections are shown.

Quantitative Polymerase Chain Reaction

For quantitative polymerase chain reaction (qPCR) total RNA extraction was performed using RNeasy mini kit (Qiagen, Venlo, the Netherlands) according to the manufacturer's instructions. Copy DNA was prepared (kit #A3500; Promega, Leiden, The Netherlands) and qPCR for C/EBP , PPAR- , KLF-5, C7orf68,ANGPTL4, ADAMTS9, SLC39A14, SRPX2 performed on the ABI-7700 system (Applied Biosystems by Thermo Fisher, Landsmeer, The Netherlands) using established primer/probe sets (Assays on Demand; Applied Biosystems by Thermo Fisher, Landsmeer, The Netherlands) and Mastermix (Eurogentec, Seraing, Belgium). Glycceraldehyde-3-phosphate dehydrogenase (GAPDH) expression was used as for reference and normalization.

Microarray

RNA extraction was performed from full thickness aortic wall samples from 31 elective and 17 ruptured AAA patients (mean age: 69.5±7.2 and 73.5±11.3 years; mean diameter 62.3±12.1 and 77.0±14.9 mm respectively) and 9 control samples (infra renal aorta obtained during kidney procurement for donation, mean age: 68.8±9 years; mean diameter 19.6±2.6mm). RNA from aneurysm wall was labeled and hybridized to Illumina HumanHT-12 v4 BeadChips. Arrays were scanned with an Illumina iScan microarray scanner. Bead level data preprocessing was done in Illumina GenomeStudio.

Analysis of array data

Quantile normalization and background reduction were performed according to standard procedures in the Illumina GenomeStudio software. Differential expression was calculated using empirical Bayes statistics included in the limma package and transcripts with an absolute log 2

fold-change ≥ 1 were considered as differentially expressed. Differentially expressed transcripts were analysed using the Ingenuity Pathway Analysis (http://www.ingenuity.com) and levels of significance were determined using Fisher's exact tests implemented in the software.

Isolation of adventitial cells

Upon medio-adventitial splitting, the adventitial matrix was digested using collagenase II solution (Worthington Biochemical, Lakewood, NJ.) according to manufacturer's instruction for a maximum of 4h with repeated resuspension. The suspension was strained through a 70-µm filter (Greiner Bio-One, Alphen aan den Rijn, The Netherlands) and centrifuged at 800rpm for 5 minutes. The precipitate was resuspended in DMEM (Gibco by Thermo Fisher, Landsmeer, The Netherlands) supplemented with 10% Fetal Bovine Serum (Sigma Aldrich, Zwijndrecht, The Netherlands) in order to inactive collagenase II activity and centrifuged at 800rpm for another 5 minutes. After cell counting using the Countess cell counter (Invitrogen by Thermo Fisher, Landsmeer, The Netherlands) cells were seeded on plastic surfaces in 6-well plates (Costar, Sigma Aldrich, Zwijndrecht, The Netherlands) at a concentration of 10^5 cells/mL in DMEM supplemented with 10% Fetal Calf Serum and 1% Penicillin/Streptomycin (Sigma Aldrich, Zwijndrecht, The Netherlands) as basal medium. Mesenchymal cellular populations were selected on their ability to adhere to plastic. Cells were passaged when they reached 70-80% confluence.

Adipogenic differentiation assay

Adipogenic differentiation potential was assessed by exposing the adventitial mesenchymal cells to an adipogenic medium.[16] In short, adhering cells were cultured to 70-80% confluence and serum starved for 48h. Next, cells were exposed to an 'adipogenic' induction medium, consisting of DMEM, 10% Fetal Calf Serum, 1700nM insulin (Sigma Aldrich, Zwijndrecht, The Netherlands), 1µM dexamethasone, and 500µM IBMX (Sigma Aldrich) for 72h. For the remainder of the experiment, cells were maintained in 'adipocyte nutrition medium' containing 2% Fetal Calf Serum, 1700nM insulin and 1µM dexamethasone. Cells were briefly formalin-fixed and fat accumulation was visualized using Oil Red O (Sigma-Aldrich, Zwijndrecht, The Netherlands) staining. Fat accumulation uptake was quantified as % of the total cell surface area covered by Oil Red O staining.

Statistical analysis

Differences in adventitial adipose tissue content were compared using the ^{2} test. Results of qPCR, Western Blotting and *in vitro* data were analyzed with Student's T-test or Wilcoxon-Mann-Whitney *U*-test to compare the different groups. Statistical significance was accepted at P<.05. All analysis were performed using the SPSS 23.0 software package (IBM Corp, Armonk, NY).

RESULTS

Clinical characteristics are shown in table 1.

The histology of a normal infrarenal aorta and popliteal artery (Figure 1A, 1B, atherosclerotic aortic tissue as reference in Supplemental Figure 1 A-E) illustrate the 3-layered vessel wall architecture with distinctive intima, media, and a loose collagenous adventitia.

Table 1. Patient Characteristics. Characteristics of patients from whom tissue was used in this study. No significant differences were present between the groups.

	Control Aorta	AAA	Control Poplitea	PAA
No. of subjects	11	31	10	15
Mean age (years)	66.36	70.94	53.60	67.80
Male gender (%)	45.45	87.10	60.00	93.33
Mean aneurysm diameter (cm)	N/A	6.32	N/A	3.19
Smoking (%)	63.64	74.19	10.00	73.33
Statin use	2	11	Unknown	2
ACE-inhibitor	1	8	Unknown	1

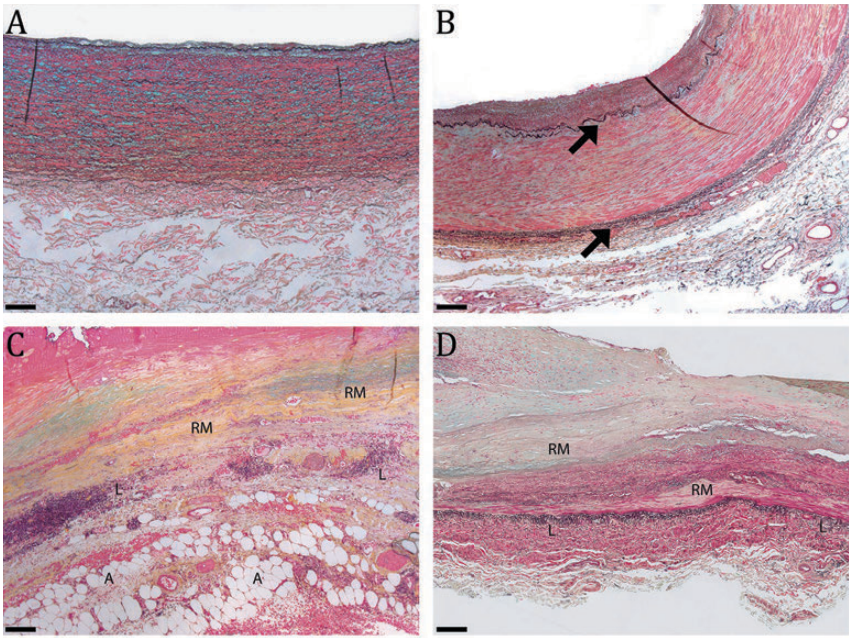

Figure 1. Histological overview of normal (non-atherosclerotic) aorta and popliteal artery and their respective aneurysms (Movat's pentachrome staining). A) healthy control aorta and B) normal popliteal artery. Multiple, parallel elastic laminae (black in Movat staining) in the normal aorta are characteristic for an elastic artery. The distinct inner and outer elastic laminae **(arrow)** of the popliteal artery characterize this artery as a muscular artery. C and D in the lower panel show representative examples of an aortic (C) and popliteal aneurysm (D). Both aneurysms show by extensive medial degradation. Prominent adventitial involvement (leucocyte infiltration **(L),** extensive matrix remodeling **(RM)** and presence of large adipocyte clusters **(A))** is characteristic for AAA. Legend to the Movat staining: Black: elastin, yellow: collagen, blue: proteoglycans, mucin, red: smooth muscle cells and fibrin, and violet: nuclei. Various shades of green reflect co-localization of collagen (yellow) and proteoglycans (blue). Mag 50x, scale bars represent 200µm. More details of the degenerative and inflammatory processes are presented in Supplemental Figure 1.

AAA wall is characterized by profound *transmural* changes with loss of the normal 3-layer architecture (Figure 1C, Supplemental Figure 1F-I). The disease is hallmarked by extensive medial elastolyis and coagulation of the medial and adventitial structures. Both layers are transformed into a condensed collagen-rich matrix, with the circular band of vasa vasora marking the former outer medial zone. The former adventitial zone contains most of the inflammatory infiltrates that characterize the disease.[1]

In sharp contrast to the AAA the 3-layer architecture is preserved in PAA. Changes appear mainly limited to the medial layer and include disruption of elastin laminae, loss of VSMCs, collagen accumulation, increased number of vasa vasora, and leucocyte infiltration. The adventitial layer appears largely preserved (Figure 1D). These observations point to adventitial involvement as the main discriminative feature between AAA and PAA.

Examination of the former adventitial zone in AAA disease revealed presence of ample adipocyte clusters in the former adventitial zone (Figure 1C, Figure 2A; Additional examples are shown in Supplemental Figure 2), illustrating that presence of adventitial adipocyte clusters is a common and extensive feature of AAA disease (P<0.0001). Although small adventitial adipocyte clusters are sporadically observed in normal aorta and PAA, the vast extent of these clusters is exclusive to AAA disease (P<.001, Figure 2B). We did not observe a correlation between AAA diameter and the adventitial adipocyte mass (r: -0.103, P = not significant).

Emergence of these adventitial clusters of adipocytes, along with extensive adventitial fibrotic changes is consistent with the process of fatty degeneration. This phenomenon links to impaired tissue regeneration and is thought to involve transdifferentiation of resident mesenchymal cells into adipocytes.[17, 18] The process of transdifferentiation critically depends on the collaborative action of transcription factors of the C/EBP family and KLF-5, and relies on PPAR-γ activity for terminal differentiation and maintenance of the adipocyte phenotype. qPCR data (Figure 3) indicates active transcription of these factors with increased in KLF-5 and PPAR-γ expression in AAA vs atherosclerotic control aorta (P<.000 and P=.032 respectively). Histological analysis (Figure 4) confirms abundant C/EBPß, KLF-5 and PPAR-γ protein expression in AAA, and shows these factors essentially, but not exclusively localize in the adventitial adipocyte clusters and mesenchymal cells, particularly those in close proximity to vasa vasora. Yet, double staining also showed expression of these factors in subsets of CD68+ macrophages. Results for Western blotting (results not shown) confirmed the above findings for C/EBPα (P=.027) and KLF-5 (P=.039). Results for PPAR-γ did not reach significance (P=.073).

All in all, these observations imply a pro-adipogenic environment in AAA disease. The adipogenic potential of AAA and control adventitial mesenchymal cells was tested by culturing these cells in adipogenic culture medium. This *in-vitro* test indicated a significantly higher adipogenic potential of AAA-derived adventitial mesenchymal cells compared control aorta to cells (P<.000; Figure 5).

An obvious next question is whether the phenomenon of fatty degeneration associates with rupture. To test the latter we compared the gene expression and the gene expression-signature of ruptured (n=17) and non-ruptured (n=31) AAA wall samples. The differential expression data for non-ruptured vs ruptured AAA shows that 5 out of the 11 most prominently upregulated, differently expressed genes in ruptured AAA are adipocyte-related (Table 2). Moreover, Ingenuity-based pathway analysis identified the adipogenesis and PPAR signaling (P=.0003 resp. 0.0026) pathways among the top-8 differentially activated canonical pathways in ruptured versus non-ruptured AAA.

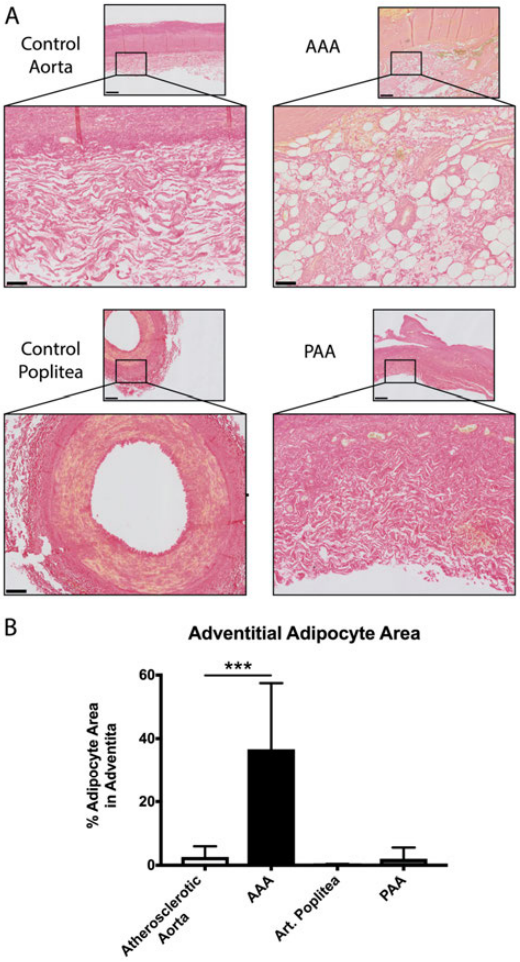

Figure 2. Adventitial adipocyte abundance is an exclusive for AAA. A) Representative images (Sirius Red) illustrating the medial-adventitial transition zone for normal aorta and popliteal artery, and their respective aneurysms. Adventitial adipocyte abundance is an exclusive feature of AAA (overview image: mag 20x, scale bar 500µm; adventitial inserts: mag 100x, scale bar 100µm). Of note: the control aorta shown is classified as end-stage atherosclerotic disease (Fibrous Calcified Plaque, Virmani classification[15]). B) Quantification of adventitial adipocyte abundance (expressed as the relative adventitial area (%) covered by adipocytes). Adventitial adipocyte abundance is an exclusive feature of AAA, ** P<0.001.

DISCUSSION

This study identifies adventitial fatty degeneration as a thus far overlooked feature of AAA disease. This observation, along with the earlier recognized fibrotic changes, typifies larger AAA as a degenerative "dystrophic" condition. Enrichment of adipocyte-related genes and pathways in ruptured AAA versus non-ruptured controls implies an association between the extent of fatty degeneration and AAA rupture.

The apparent paradox between preclinical successes of anti-inflammatory/anti-proteolytic strategies in the context of AAA disease and clinical reality implies a translational gap.[10] This gap

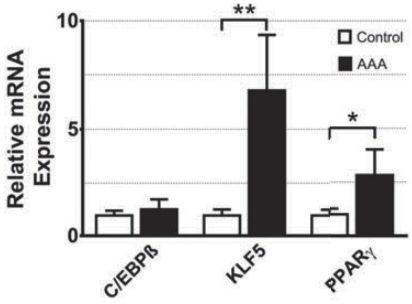

Figure 3. Aortic wall mRNA expression of adipogenic transcription factors. Relative mRNA (control aorta = 1) expression for C/EBPß, KLF-5 and PPAR-γ in control aorta and AAA. * P<0.05, ** P<0.01; %. (semi-quantitative real-time PCR, control n=10; AAA n=10).

between available models of AAA disease and the actual disease is further illustrated by failure of the experimental models to progress to rupture (of note: while rupture is a common feature of the angiotensin model, it is now clear that this model reflects a process of aortic dissection rather than of AAA disease[19, 20]).

Apparent failure of the experimental models to progress to rupture implies the chain of events leading up to rupture as a distinct entity within the disease process. Such a concept is supported by the divergence of several risk factors for AAA growth and rupture, as well as contrasting rupture risks of AAA and PAA.[13, 21, 22] In search of auxiliary processes contributing to (terminal) AAA wall weakening, we considered a re-evaluation of histo-pathological aspects of abdominal aortic and popliteal aneurysms relevant. Particular attention was paid to the adventitial structures since Hurks et al. identified extensive adventitial involvement in AAA as a clear contrasting feature between AAA and PAA.[23]

Our re-evaluation confirms preservation of adventitial structures in PAA,[23] and extensive transmural remodeling and adventitial involvement in AAA disease. A remarkable, and to the best of our knowledge, novel observation for AAA disease is the abundance of isolated adipocyte islands within the former adventitial zone. Although isolated clusters of adipocytes are occasionally found in PAA and atherosclerotic control aortas, the extent of the phenomenon is unique to AAA.

Adventitial adipocyte abundance in AAA could be the consequence of a passive process in which vanished adventitial matrix structures are replaced by peri-aortic adipose tissue. Such a phenomenon would imply continuity of the adipose islands with the per-aortic adipose tissue, which is clearly not the case. Moreover, strict confinement of the process to the former adventitia, the large adipocyte cell volume, and intertwining strands of matrix in between the adipocyte clusters are not consistent with a simple passive replacement mechanism.

An alternative explanation for the adipocyte abundance is the process of fatty (adipogenic) degeneration. Fatty degeneration is a well-known phenomenon in chronic degenerative conditions such as severe limb ischemia, muscle wasting dystrophies, and recurrent rotator cuff lesions.[17, 18, 24] The phenomenon is thought to reflect dysregulated repair processes that also include (trans) differentiation of mesenchymal cells into adipocytes.[18, 25]

The process of adipogenic transdifferentiation relies on the availability of transcription factors from the C/EBP and KLF-family families and presence of the nuclear receptor PPAR-γ[26-28] with

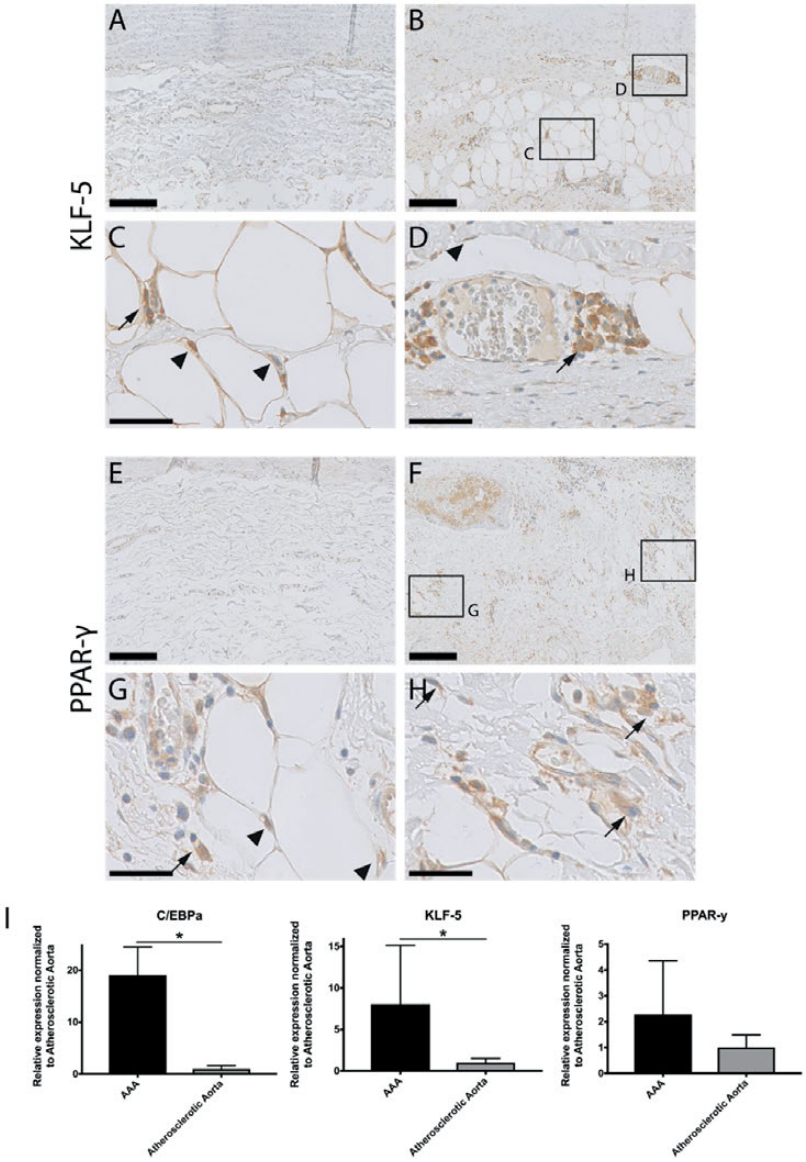

Figure 4. Tissue distribution (immunohistochemistry)of pro-adipogenic transcription factors in AAA. Immunohistochemical staining for KLF-5 and PPAR-γ. A) Minimal KLF-5 expression in control aorta. B,C,D) Abundant KLF in AAA in adipocytes (arrow heads) and in mesenchymal cells (arrows in C and D) in the vicinity of vasa vasora and near the adipocyte clusters. E) minimal PPAR-γ expression in control aorta. F,G,H) PPAR-γ expression follows a similar expression pattern to KLF-5 being expressed in adipocytes (arrowheads) and 'mesenchymal' cells (arrows G and H). A,B,E,F mag 50x, scale bar 200μm; C,D,G,H mag 400x scale bar 50μm. I) Relative C/EBPα, KLF-5 and PPAR-γ protein expression (data normalized to α-actin) in AAA (solid bars) and atherosclerotic control aorta (grey bars). *P=.027 (C/EBPα) resp. 0.039 (KLF-5).

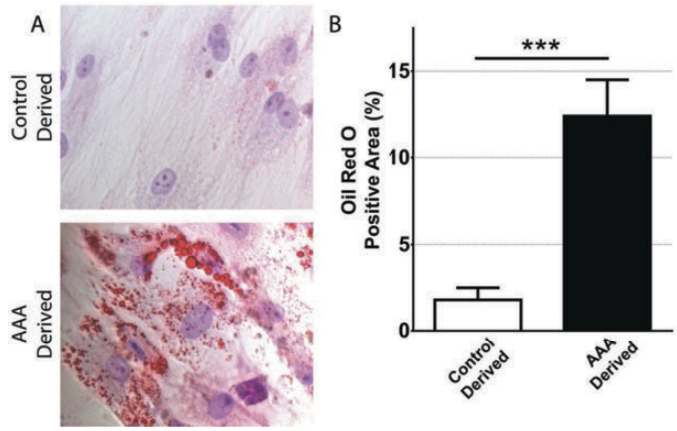

Figure 5. Increased adipogenic potential of AAA-derived mesenchymal cells. A) Representative images (Oil-Red-O) illustrating fat accumulation in cultured aortic mesenchymal cells after 14 days of in-vitro culture. Minimal accumulation is seen in control aorta-derived mesenchymal cells (upper panel). Extensive fat accumulation is seen in AAA- cells (lower panel) (Mag 400x). B) Quantitative analysis of Oil-red-O staining. Significantly higher fat accumulation in AAA-derived mesenchymal cells (* P<0.000; Control derived (n=6); AAA derived (n=6)).

Table 2. Microarray analysis of elective and ruptured AAA. Adipocyte-associated genes dominate the top 11 most differentially upregulated genes in ruptured (n=17) vs. stable AAA (n=31).

Gene	Fold Up Array	P Value Array	Rank in top 11	P Value PCR-validation
C7orf68	412	<0.000	1	<0.000
ANGPTL4	226	<0.000	2	<0.000
ADAMTS9	126	<0.000	5	0.0006
SLC39A14	107	<0.000	7	0.092*
SRPX2	74	<0.000	11	0.0029

*Number of transcripts just above the detection limit of the PCR

sustained expression of PPAR-γ as prerequisite for maintaining the adipocyte phenotype.[26, 28] We confirmed abundant C/EBPß, KLF-5 and PPAR-γ presence in the mesenchymal cells of the outer media and adventitia of the aneurysm wall, showing the transcriptional machinery required for fatty degeneration is present within mesenchymal cells of the AAA wall and co-localizes with the adipocyte clusters.

The process of fatty degeneration further depends on the ability of the resident mesenchymal cell population to undergo trans-differentiation into adipocytes. *In vitro* differentiation assays confirmed their adipogenic potential and indicated a significantly higher adipogenic potential for AAA-derived mesenchymal cells. This phenomenon implies intrinsic differences between control and AAA-derived mesenchymal cells. The persistence of the intrinsic differences *in vitro* ('priming' phenomenon) may hint at epigenetic reprogramming of AAA mesenchymal cells secondary to micro-environmental changes such as matrix properties and the growth factor/cytokine milieu.[26, 29]

Extensive adventitial fatty degeneration appears unique to AAA, and discriminates AAA from PAA disease. Reported associations between adventitial triglyceride content and AAA diameter suggest an association between the extent of fatty degeneration and disease progression.[30] As such it may contribute to the debilitation processes leading up to rupture.[1] To test the latter we analysed the data from a genome wide analysis of genes expressed in sized-matched stable and ruptured AAA. The clear enrichment of adipocyte-specific genes and the molecular pathways related to adipose tissue in ruptured AAA is consistent with increased adipogenic degeneration in ruptured AAA.

It came to our attention that quantifying the extent of fatty degeneration could contribute to an improved rupture risk estimation in patients with larger AAA. Unfortunately, although MRI provides an excellent distinction between adipose and surrounding tissue, we concluded that the infra-renal abdominal aorta is not easily accessible for the high-resolution level of imaging required for quantifying the extent adventitial fatty degeneration.

A possible role of a fatty degeneration in terminal aorta weakening may have major implications for the use of PPAR-γ agonists in AAA patients. Recent studies propose PPAR-γ activation as a means of attenuating AAA growth and preventing rupture.[31,32] Indeed, PPAR-γ agonists quench vascular inflammation in both humans and small animals, and reduce AAA growth in different animal models.[31, 33, 34] Moreover, it has been suggested that PPAR-γ signaling is crucial for the integrity of elastic fibers in mice protecting against aortic dilatation.[32] Yet, as fatty degeneration is not a feature of these animal models, potential negative aspects of PPAR-γ activation may be missed. Over and above, our data implies abundant PPAR- expression in AAA wall samples, an observation consistent with comprehensive endogenous activation of the pathway. It is thus questionable whether additional exogenous PPAR-γ activation will beneficially influence inflammation in and the progression of AAA.

Our observations rely on the availability of human AAA material. As a consequence all conclusions are based on surgical samples representing end-stage human disease. As adipogenic degeneration is not a feature in animal models of the disease, we were unable to examine the timing and role of adipogenic degeneration during AAA progression. A re-evaluation of histological images published by other groups also revealed the phenomenon of fatty degeneration; showing adventitial adipogenic degeneration is a universal phenomenon of AAA disease (Supplemental figure 4).[23, 35-37] Moreover, our studies rely on the availability of surgical specimens. In era of EVAR dominance for elective repair, wall surgical specimens are getting rare. As such our study is based on older material and the level of statin use is below current standards.

REFERENCES

1. Thompson RW, Geraghty PJ, Lee JK. Abdominal aortic aneurysms: Basic mechanisms and clinical implications. *Current problems in surgery*. 2002;39:110-230
2. Sakalihasan N, Limet R, Defawe OD. Abdominal aortic aneurysm. *Lancet*. 2005;365:1577-1589
3. Abdul-Hussien H, Hanemaaijer R, Kleemann R, Verhaaren BF, van Bockel JH, Lindeman JH. The pathophysiology of abdominal aortic aneurysm growth: Corresponding and discordant inflammatory and proteolytic processes in abdominal aortic and popliteal artery aneurysms. *Journal of vascular surgery*. 2010;51:1479-1487
4. Lindeman JH. The pathophysiologic basis of abdominal aortic aneurysm progression: A critical appraisal. *Expert Rev Cardiovasc Ther*. 2015;13:839-851
5. Bigatel DA, Elmore JR, Carey DJ, Cizmeci-Smith G, Franklin DP, Youkey JR. The matrix metalloproteinase inhibitor bb-94 limits expansion of experimental abdominal aortic aneurysms. *Journal of vascular surgery*. 1999;29:130-138; discussion 138-139
6. Kalyanasundaram A, Elmore JR, Manazer JR, Golden A, Franklin DP, Galt SW, *et al*. Simvastatin suppresses experimental aortic aneurysm expansion. *Journal of vascular surgery*. 2006;43:117-124
7. Miyake T, Aoki M, Osako MK, Shimamura M, Nakagami H, Morishita R. Systemic administration of ribbon-type decoy oligodeoxynucleotide against nuclear factor kappab and ets prevents abdominal aortic aneurysm in rat model. *Mol Ther*. 2011;19:181-187
8. Parodi FE, Mao D, Ennis TL, Bartoli MA, Thompson RW. Suppression of experimental abdominal aortic aneurysms in mice by treatment with pyrrolidine dithiocarbamate, an antioxidant inhibitor of nuclear factor-kappab. *Journal of vascular surgery*. 2005;41:479-489
9. Steinmetz EF, Buckley C, Shames ML, Ennis TL, Vanvickle-Chavez SJ, Mao D, *et al*. Treatment with simvastatin suppresses the development of experimental abdominal aortic aneurysms in normal and hypercholesterolemic mice. *Annals of surgery*. 2005;241:92-101
10. Kokje VB, Hamming JF, Lindeman JH. Pharmaceutical management of small abdominal aortic aneurysms: A systematic review of the clinical evidence. *Eur J Vasc Endovasc Surg*. 2015
11. Englesbe MJ, Wu AH, Clowes AW, Zierler RE. The prevalence and natural history of aortic aneurysms in heart and abdominal organ transplant patients. *Journal of vascular surgery*. 2003;37:27-31
12. Lindeman JH, Rabelink TJ, van Bockel JH. Immunosuppression and the abdominal aortic aneurysm: Doctor jekyll or mister hyde? *Circulation*. 2011;124:e463-465
13. Van Bockel J.H., Hamming JF. Lower extremity aneurysms. In: R.B. R, ed. *Vascular surgery*. Phildelphia, PA: Elsevier Saunders; 2005:1534-1551.
14. van Dijk RA, Virmani R, von der Thusen JH, Schaapherder AF, Lindeman JH. The natural history of aortic atherosclerosis: A systematic histopathological evaluation of the peri-renal region. *Atherosclerosis*. 2010;210:100-106
15. Virmani R, Kolodgie FD, Burke AP, Farb A, Schwartz SM. Lessons from sudden coronary death: A comprehensive morphological classification scheme for atherosclerotic lesions. *Arteriosclerosis, thrombosis, and vascular biology*. 2000;20:1262-1275
16. Scott MA, Nguyen VT, Levi B, James AW. Current methods of adipogenic differentiation of mesenchymal stem cells. *Stem cells and development*. 2011;20:1793-1804
17. Kang JR, Gupta R. Mechanisms of fatty degeneration in massive rotator cuff tears. *J Shoulder Elbow Surg* 2012;21:175-180
18. Rodeheffer MS. Tipping the scale: Muscle versus fat. *Nature cell biology*. 2010;12:102-104
19. Saraff K, Babamusta F, Cassis LA, Daugherty A. Aortic dissection precedes formation of aneurysms and atherosclerosis in angiotensin ii-infused, apolipoprotein e-deficient mice.

Arteriosclerosis, thrombosis, and vascular biology. 2003;23:1621-1626

20. Trachet B, Fraga-Silva RA, Piersigilli A, Tedgui A, Sordet-Dessimoz J, Astolfo A, *et al*. Dissecting abdominal aortic aneurysm in ang ii-infused mice: Suprarenal branch ruptures and apparent luminal dilatation. *Cardiovascular research*. 2015;105:213-222

21. Thompson SG, Brown LC, Sweeting MJ, Bown MJ, Kim LG, Glover MJ, *et al*. Systematic review and meta-analysis of the growth and rupture rates of small abdominal aortic aneurysms: Implications for surveillance intervals and their cost-effectiveness. *Health Technol Assess*. 2013;17:1-118

22. Gokani VJ, Sidloff D, Bath MF, Bown MJ, Sayers RD, Choke E. A retrospective study: Factors associated with the risk of abdominal aortic aneurysm rupture. *Vascul Pharmacol*. 2015;65-66:13-16

23. Hurks R, Kropman RH, Pennekamp CW, Hoefer IE, de Vries JP, Pasterkamp G, *et al*. Popliteal artery aneurysms differ from abdominal aortic aneurysms in cellular topography and inflammatory markers. *Journal of vascular surgery*. 2014;60:1514-1519

24. Weiss DJ, Casale GP, Koutakis P, Nella AA, Swanson SA, Zhu Z, *et al*. Oxidative damage and myofiber degeneration in the gastrocnemius of patients with peripheral arterial disease. *Journal of translational medicine*. 2013;11:230

25. Joe AW, Yi L, Natarajan A, Le Grand F, So L, Wang J, *et al*. Muscle injury activates resident fibro/adipogenic progenitors that facilitate myogenesis. *Nature cell biology*. 2010;12:153-163

26. Cristancho AG, Lazar MA. Forming functional fat: A growing understanding of adipocyte differentiation. *Nature reviews. Molecular cell biology*. 2011;12:722-734

27. Oishi Y, Manabe I, Tobe K, Tsushima K, Shindo T, Fujiu K, *et al*. Kruppel-like transcription factor klf5 is a key regulator of adipocyte differentiation. *Cell metabolism*. 2005;1:27-39

28. Farmer SR. Transcriptional control of adipocyte formation. *Cell metabolism*. 2006;4:263-273

29. Steger DJ, Grant GR, Schupp M, Tomaru T, Lefterova MI, Schug J, *et al*. Propagation of adipogenic signals through an epigenomic transition state. *Genes & development*. 2010;24:1035-1044

30. Kugo H, Zaima N, Tanaka H, Mouri Y, Yanagimoto K, Hayamizu K, *et al*. Adipocyte in vascular wall can induce the rupture of abdominal aortic aneurysm. *Scientific reports*. 2016;6:31268

31. Motoki T, Kurobe H, Hirata Y, Nakayama T, Kinoshita H, Rocco KA, *et al*. Ppar-gamma agonist attenuates inflammation in aortic aneurysm patients. *Gen Thorac Cardiovasc Surg*. 2015;63:565-571

32. Tai HC, Tsai PJ, Chen JY, Lai CH, Wang KC, Teng SH, *et al*. Peroxisome proliferator-activated receptor gamma level contributes to structural integrity and component production of elastic fibers in the aorta. *Hypertension*. 2016

33. Hasan DM, Starke RM, Gu H, Wilson K, Chu Y, Chalouhi N, *et al*. Smooth muscle peroxisome proliferator-activated receptor gamma plays a critical role in formation and rupture of cerebral aneurysms in mice in vivo. *Hypertension*. 2015;66:211-220

34. Jones A, Deb R, Torsney E, Howe F, Dunkley M, Gnaneswaran Y, *et al*. Rosiglitazone reduces the development and rupture of experimental aortic aneurysms. *Circulation*. 2009;119:3125-3132

35. Hinterseher I, Schworer CM, Lillvis JH, Stahl E, Erdman R, Gatalica Z, *et al*. Immunohistochemical analysis of the natural killer cell cytotoxicity pathway in human abdominal aortic aneurysms. *International journal of molecular sciences*. 2015;16:11196-11212

36. Golledge J, Muller J, Shephard N, Clancy P, Smallwood L, Moran C, *et al*. Association between osteopontin and human abdominal aortic aneurysm. *Arteriosclerosis, thrombosis, and vascular biology*. 2007;27:655-660

37. Hurks R, Vink A, Hoefer IE, de Vries JP, Schoneveld AH, Schermerhorn ML, *et al*. Atherosclerotic risk factors and atherosclerotic postoperative events are associated with low inflammation in abdominal aortic aneurysms. *Atherosclerosis*. 2014;235:632-641

SUPPLEMENTAL DATA

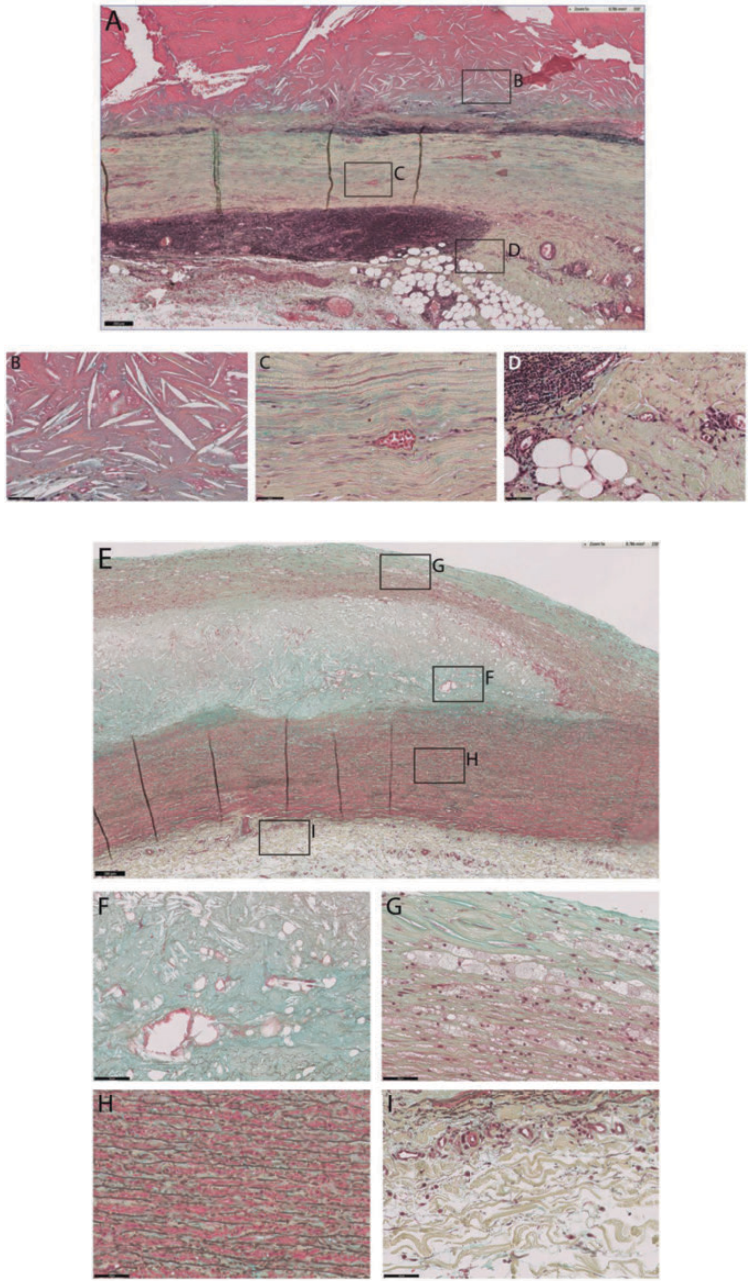

Supplemental Figure 1. Movat's pentachrome staining illustrating the distinctive histomorphologies of atherosclerotic control abdominal aorta (A) and AAA tissue (B). (A) The intimal layer of atherosclerotic aorta tissue is hallmarked by the presence of an atherosclerotic lesion (presented lesion: late fibroatheroma (Virmani classification[15])). The lesion is characterized by presence of necrotic core with cholesterol crystals (arrow) (A-I).

- The core is covered by a so called fibrous cap (A-II). Foam-cells present in the cap are marked (*). A detail of the intact media underlying the atherosclerotic lesion is shown in A-III. The medial layer consists of multiple, uninterrupted lamellar units of elastin sheets with interspersed vascular smooth muscle cells. The adventitia (A-IV) consists of a loose collagenous network and harbors a vascular plexus (vasa vasora, indicated by the open triangles) at the medial-adventitial border. (B) shows the histo-morphology of an AAA. Note loss of typical 3-layer structure. The initma is covered by remnants of the luminal thrombus (fibrin is stains red in the Movat staining). Of note: the large basal cholesterol clefts (indicated by the arrows in B-I) at the basis of the thrombus presumably reflect cholesterol accumulation from trapped erythrocyte membranes. In the AAA, the intimal and medial layers are transformed into a condensed collagenous, vascular smooth muscle cell/proteoglycan-poor matrix ("fibrotic matrix", B-II). The zone harboring the vasa vasora (indicated by triangles in overview and detail B-II) remains as a landmark, marking the former medial-adventitial border zone (bz). The former adventitia (B-III) shows areas of fibrosis inter-dispersed with adipocyte clusters and is home to tertiary follicles (tf).

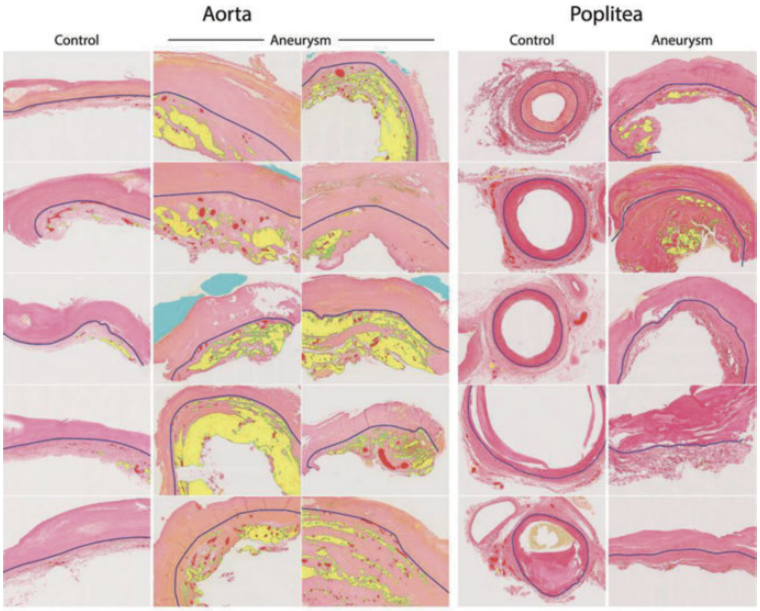

Supplemental Figure 2. Overview of adipocyte distribution within the adventitial layer. All images oriented with luminal side up (unless the whole lumen is visible). Adventitia is defined as area under the blue line with the yellow overlay representing all adventitial adipocytes and the red overlay representing all adventitial vasa vasora. Light blue overlay indicates adhering luminal thrombus. Mag 20x.

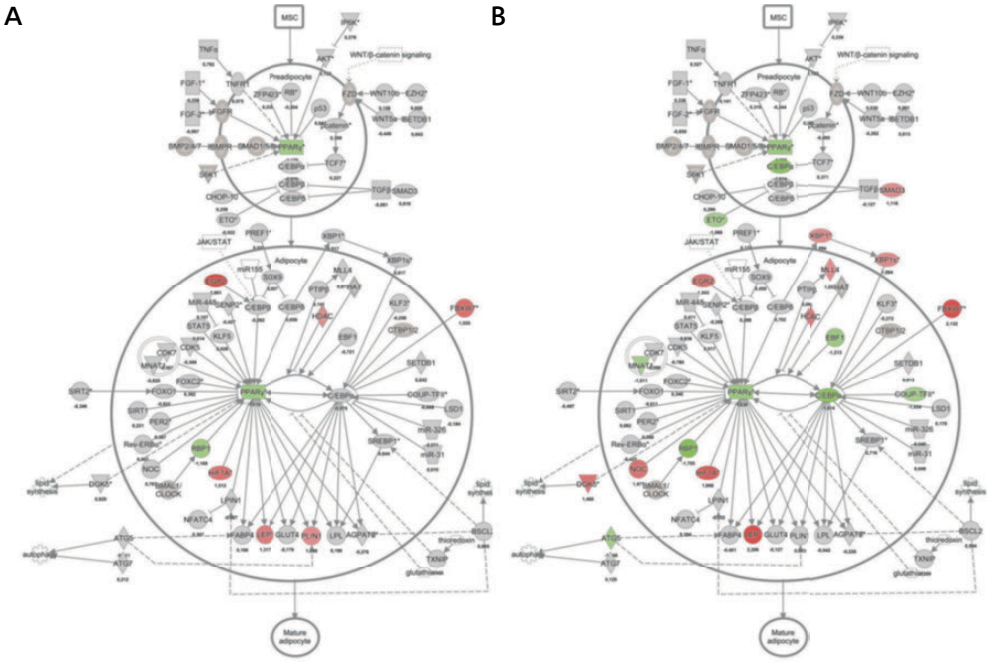

Supplemental Figure 3. Comparison of adipogenesis pathway on microarray between ruptured and elective AAA. Pathways analysis (Ingenuity Pathway Analysis) showing activation of the adipogenesis network in respectively ruptured (sFigure 3A; n=17) and stable (electively operated, (sFigure 3B; n=31)) aneurysm wall samples using atherosclerotic controls (n=10) as reference. Green overlay = downregulation; Red overlay = upregulation.

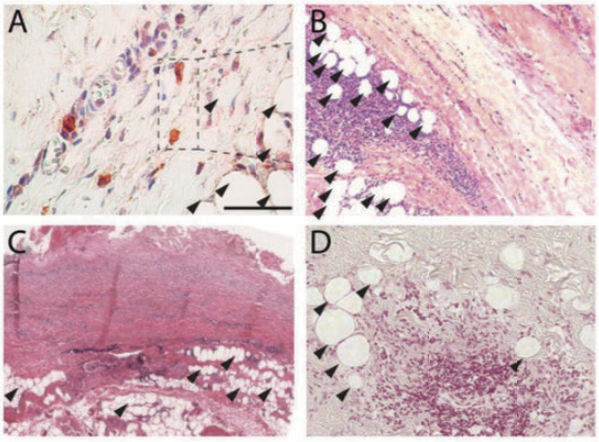

Supplemental Figure 4. Overview of histological images from previous publications showing adventitial fatty degeneration in AAA samples. Fatty degeneration can also be appreciated in earlier publications: A) Hinterseher, Int J Mol Sci 2015[35]; B) Golledge, ATVB 2007[36]; C) Hurks, Atherosclerosis 2014[37]; D) Hurks, JVS 2014[23]. Arrowheads denote adipocytes within the matrix of human AAA, illustrating adventitial adipogenic degeneration is a common phenomenon in AAA.